Subseasonal organization of ocean chlorophyll: Prospects for prediction based on the Madden-Julian Oscillation

Duane E. Waliser,[1] Ragu Murtugudde,[2] Peter Strutton,[3] and Jui-Lin Li[1]

Received 4 August 2005; revised 21 October 2005; accepted 27 October 2005; published 3 December 2005.

[1] Analysis of satellite ocean color and rainfall data shows that the Madden-Julian Oscillation (MJO) produces systematic and significant variations in ocean surface Chlorophyll (Chl) in a number of regions across the tropical Indian and Pacific Oceans, including the northern Indian Ocean, a broad expanse of the northwestern tropical Pacific Ocean, and a number of near-coastal areas in the far eastern Pacific Ocean. Potential mechanisms for this modulation are examined with the result that wind-induced vertical entrainment at the base of the ocean mixed layer appears to play an important role. Given evidence that the MJO is predictable with 2–3 week lead-times, surface Chl may also be predictable at similar lead times with implications for the fishing industry and public health sectors concerned with cholera epidemics. **Citation:** Waliser, D. E., R. Murtugudde, P. Strutton, and J.-L. Li (2005), Subseasonal organization of ocean chlorophyll: Prospects for prediction based on the Madden-Julian Oscillation, *Geophys. Res. Lett.*, *32*, L23602, doi:10.1029/2005GL024300.

1. Introduction

[2] Interest in tropical intraseasonal variability (TISV) has intensified in recent years due the important role it plays in connecting the better understood weather and seasonal-to-interannual climate variations [*Lau and Waliser*, 2005]. The most notable form of TISV is the Madden-Julian Oscillation (MJO) which is characterized by large-scale eastward-propagating disturbances in the tropics [*Hendon and Salby*, 1994; *Madden and Julian*, 1994]. Numerous interactions between the MJO and other weather/climate processes have been described. These include the onsets and breaks of the Asian-Australian monsoon, the evolution of El Niño/La Niña and the character and strength of higher frequency tropical variability, including the diurnal cycle, tropical cyclones, and extreme precipitation events. The influences on higher frequency variability even extend to the extratropical circulation and its weather patterns. Through its modulation of surface momentum and heat fluxes, the MJO can produce significant and systematic variations in sea surface temperature (SST) [*Hendon and Glick*, 1997; *Kemball-Cook and Wang*, 2001], surface mixed layer depth, and equatorial/coastal current and wave activity [*Hendon et al.*, 1998; *Waliser et al.*, 2003a]. These interactions, particularly those related to mixed-layer variations and SST, have been postulated [*Waliser et al.*, 1999; *Fu et al.*, 2003; *Zheng et al.*, 2004] to be important to the MJO phenomenon by providing a feedback to the atmosphere which influences a number of fundamental characteristics of the MJO.

[3] In this study, we explore a new area of MJO impacts, namely its influence on ocean biology. Our study framework is motivated by the following considerations: (1) ocean Chlorophyll (Chl) represents a measure of biomass at the lowest levels of the ocean food chain, and at least at lower frequencies is shown to affect top predators such as fish [*Lehodey et al.*, 1997; *Chavez et al.*, 2003], (2) surface Chl is an indicator of conditions conducive to the presence of cholera in coastal zones [*Colwell*, 1996; *Pascual et al.*, 2000], (3) the MJO modulates physical properties of the atmosphere and near-surface ocean that have been shown to influence the distribution of Chl at synoptic and interannual time scales [*Murtugudde et al.*, 1999; *Strutton and Chavez*, 2000], and (4) the MJO has been shown to be predictable with lead times of 2–3 weeks [*Waliser et al.*, 2003b]. Given the above, we explore the relationship between the MJO and the distribution of ocean surface Chl.

2. Data and Methods

[4] Atmospheric conditions associated with the MJO were identified using an extended Empirical Orthogonal Function (EEOF) analysis of 35–95 day band-passed pentad rainfall data (based on the work by *Xie and Arkin* [1997]) that extends from 1979–2003. The filtered data were separated into boreal winter (Nov–Apr) and summer (May–Oct). For each season, EEOFs were computed for ±5 pentad time lags on the region between 30°N–30°S and 30°E–180°E. The boreal winter mode 1 pattern represents an eastward propagating structure with about a 50-day period that is strongly reminiscent of the boreal winter MJO while the boreal summer mode 1 pattern exhibits significant northward propagation as well (e.g., Figure 1, discussed further below). Plots of these EEOFs for nearly identical constructions of the boreal winter MJO structures are given by *Waliser et al.* [2003a], along with more discussion of this EEOF and compositing framework.

[5] To construct a canonical structure of the MJO and associated ocean forcing components, observed MJO events were selected when the value of the unit-normalized amplitude time series of EEOF mode 1 exceeded 1.0. The selected events were averaged to form a composite MJO. This was performed separately for summer and winter for the rainfall data mentioned above (i.e. 1979–2003), as well as (1988–1999) pentad resolution SSM/I-based surface wind data [*Atlas et al.*, 1996] and July 1983 to June 1991

[1]Jet Propulsion Laboratory, California Institute of Technology, Pasadena, California, USA.
[2]Earth System Science Interdisciplinary Center, University of Maryland, College Park, Maryland, USA.
[3]College of Oceanic and Atmospheric Sciences, Oregon State University, Corvallis, Oregon, USA.

0094-8276/05/2005GL024300$05.00

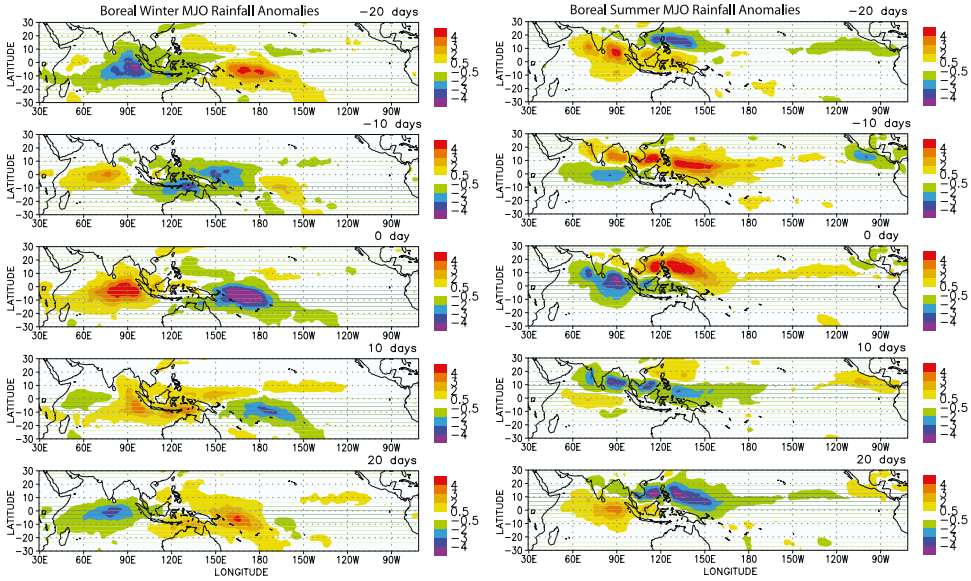

Figure 1. Composite boreal winter (left) and summer (right) MJO rainfall (mm day^{-1}) patterns.

ISCCP-based surface shortwave data [*Bishop et al.*, 1997]. For rainfall, shortwave and wind, this involved 51 [49], 10 [14], and 16 [21] events, respectively for the summer [winter] composite event. To succinctly illustrate these composites, weighted means of the 11-pentad composite were performed by applying a 1-2-1 average on the −5, −4 and −3 pentad lag maps (labeled "−20 days"), the −3, −2, and −1 pentad lag maps (labeled "−10 days"), and so forth.

[6] To construct the composite for ocean surface Chl, the daily, 9 km mapped images of SeaWiFS (V4) Chl [*McClain et al.*, 2004] were obtained for the 55-day periods corresponding to each of the MJO events that overlap the SeaWiFS record. This amounts to 13 (14) boreal summer (winter) events. In this case, the corresponding 5-panel composites were constructed by averaging the five 11-day sequences within the 55-day events. For example, the earliest 11 days corresponds to −20 day lag, the middle 11 days corresponds to 0 day lag, etc. In this case then, the number of daily samples in each summer (winter) map can, depending on cloudiness, range up to 11 times 13 (14). Note that the Chl, as well as the other data sets, were mapped onto a common 1° × 1° grid. To focus on the modulations of Chl over the MJO cycle, these Chl maps were normalized by the "seasonal" means (not shown)(Seasonal and monthly Chl maps are available at oceancolor.gsfc.nasa.gov). In this case, the seasonal means were constructed by computing the mean of all the Chl maps associated with the selected winter and summer MJO events, respectively (i.e. maximum N = 55 days * 13 [14] events = 715 [770] for summer [winter], respectively).

3. Results

[7] Figure 1 (left) illustrates a typical boreal winter MJO event. At a lag of −20 days, a positive rainfall anomaly forms over the far western Indian Ocean (IO), and over the following 40–50 days, intensifies and propagates eastward to the central Pacific Ocean (PO). In the Indian and west Pacific oceans, where the SST is relatively warm, the MJO interacts strongly with the upper-level atmospheric flow, cloud field, surface winds and heat fluxes. Once the disturbance reaches the date line, and thus cooler SSTs, convection subsides and the disturbance continues largely confined to the upper tropospheric wind field. During the boreal summer, the change in the large-scale circulation associated with the Asian summer monsoon results in the disturbances propagating northeastward. Figure 1 (right) illustrates the evolution of the rainfall anomaly associated with a typical boreal summer MJO event. These maps are consistent with typical MJO variability and its seasonal modulation [*Waliser*, 2005].

[8] Figure 2 shows the corresponding maps for ocean surface Chl distributions relative to their seasonal means. Values of 0.8 and 1.2 represent a Chl value that is 80% and 120% of the seasonal mean, respectively. Widespread modulation of Chl is evident over many parts of the IO and PO. In the boreal winter, Chl anomalies occur in the northwest IO, including the southern tip of India, as well as areas of the northwest, central and far eastern PO. In the boreal summer, the largest and most systematic Chl variations occur in the northern IO, around S.E. Asia, over a broad region of the western/central PO, and a number of coastal areas in the far eastern PO. The boreal winter variations in the eastern PO do not appear quite as robust as those for the boreal summer, except possibly along the west coast of Mexico.

[9] To illustrate the phase and magnitude of these variations in relation to the MJO-related surface solar and wind speed anomalies, as well as highlight their statistical significance, the data are averaged over a few select regions (see boxes in Figure 2) and plotted versus time lag in Figure 3. In this case, the Chl values were calculated by averaging the number of available 1° × 1° samples within the given rectangular region, over the number of MJO events selected, over the 11 days for each part of the cycle shown, then normalizing by the seasonal mean. For example, if the rectangle was 10° × 10°, then the number of samples

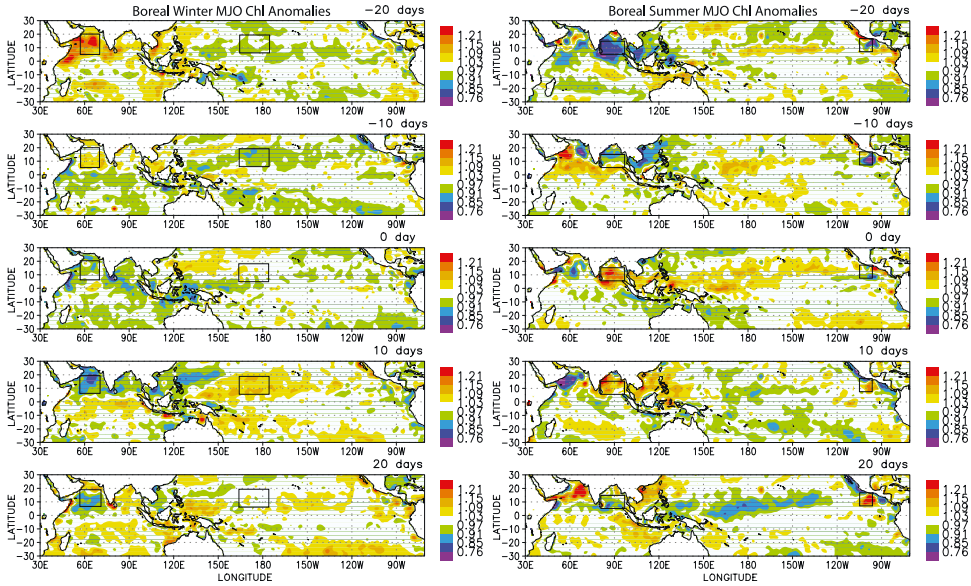

Figure 2. Same as Figure 1, except for ocean surface Chl with values are normalized by the seasonal mean.

ranges up to 100 (grid points) times 14 (events, in the case of summer) times 11 days, which is equal to 15400. However, the number would typically be less due the presence of clouds, although based on the values and error bars in Figure 3 is still large enough to adequately sample the "cloudy" regime of the MJO due to the high spatial resolution of the data (O(km)) and the multi-day averaging. For the mean values shown in Figure 3, the number of samples ranges between about 5–30 $\times$ 10^3. The degrees of freedom for the calculation of the error bars (95% significance) were computed by taking the number of samples and dividing by 8, where the latter accounts for an approximate autocorrelation of Chl in time of 2 days and in latitude and longitude of 2 degrees. Examining of the Chl variations for the four select regions – the Arabian Sea and the western PO for winter and the Bay of Bengal and far eastern PO for summer – shows that high anomalies (~110–115%) are statistically distinct from the low anomalies (~85–90%). Moreover, the typical peak-to-peak variations that occur over the course of about 25 days are on the order of 25–30% of the seasonal mean.

[10] Along with Chl, the plots in Figure 3 also illustrate the anomalous variations in surface shortwave radiation - which are roughly inversely proportional to the rainfall variations – and surface wind speed. In the Arabian Sea in winter and Bay of Bengal in summer, there is some evidence that the solar radiation is in phase or slightly leads the variations in Chl. The two other regions shown are almost out of phase with surface shortwave, likely because variability in primary productivity in these regions is almost certainly not light-driven. Surface wind speed in 3 of the 4 regions exhibits a positive relationship to Chl with wind speed slightly leading Chl. It is likely that wind speed is a surrogate for entrainment of nutrient-rich water into the mixed-layer from below [e.g., *Siegel et al.*, 1995]. Additional support for this comes from our examination of the phasing between the Chl values and model-derived ocean mixed-layer depth anomalies [*Waliser et al.*, 2003a], which indicated a similar relation. In the Arabian Sea, Chl and wind speed anomalies have an inverse relationship. In this upwelling-dominated system, wind-stress curl and Ekman pumping are more important through their impact on the thermocline/nutricline depth [*Wiggert et al.*, 2002]. In addition to these processes, other mechanisms that need to be investigated include the influence of changing winds on horizontal advection, and the deposition of dust (a source of

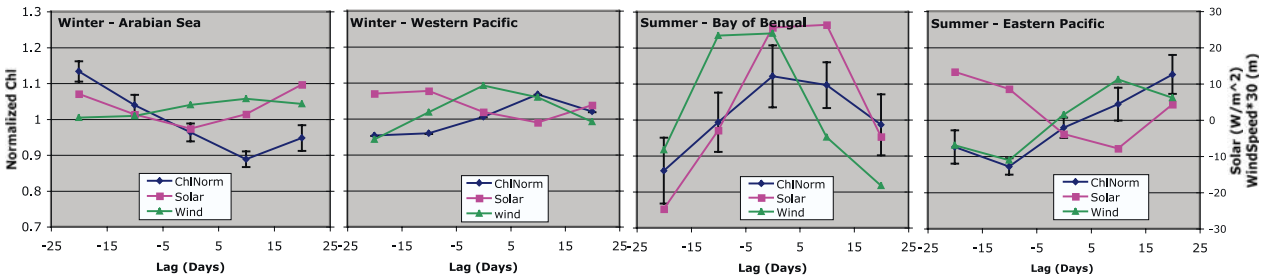

Figure 3. Domain-averaged values of normalized Chl (blue), surface solar insolation anomaly (magenta), and surface wind speed anomaly (green). The domains are illustrated as boxes in Figure 2 and are 5–20N, 55–70E and 5–20N, 165E–170W for winter, 5–15N, 80–100E and 5–15N, 105–95W for summer. Chl error bars are 95% confidence limits – bars are too small to see on second plot.

iron) from nearby land masses [*McCreary et al.*, 2001; *Wiggert et al.*, 2002].

4. Summary

[11] Previous work has documented the coupling between the MJO and variability in SST. Here, we have quantified the relationship between the MJO and Chl. Given the importance of Chl in determining the heat budget of the near-equatorial mixed layer, these results might represent a second order feedback to the temperature evolution of the surface ocean [*Nakamoto et al.*, 2001; *Murtugudde et al.*, 2002], and, in turn to atmospheric MJO processes [*Gildor et al.*, 2003]. In addition, the existence of a systematic modulation of Chl, along with the knowledge that the MJO is predictable at lead times of 2 weeks or more, implies that tropical Chl might be also predictable with similar lead times. This combined with Chl's relation to higher trophic-level productivity [*Lehodey et al.*, 2003], could lead to predictive capabilities for fish abundance. Further analysis is underway to explore]the fisheries response to Chl variability at MJO time-scales. The use of remote sensing for detection of *Vibrio cholerae*, the bacterium that causes cholera in humans, has been shown to be possible [*Lobitz et al.*, 2000] even though the predictive aspects were not known thus far. This study provides the first such climate linkage with clear potential for preventive action.

[12] **Acknowledgments.** Support was provided by NASA, NOAA and JPL's HRDF and RTD programs. The Chl data were provided by the SeaWiFS Project and NASA's DAAC.

References

Atlas, R., R. N. Hoffman, S. C. Bloom, J. C. Jusem, and J. Ardizzone (1996), A multiyear global surface wind velocity dataset using SSM/I wind observations, *Bull. Am. Meteorol. Soc.*, *77*, 869–882.

Bishop, J. K. B., W. B. Rossow, and E. G. Dutton (1997), Surface solar irradiance from the International Satellite Cloud Climatology Project 1983–1991, *J. Geophys. Res.*, *102*, 6883–6910.

Chavez, F. P., J. Ryan, S. E. Lluch-Cota, and M. Niquen (2003), From anchovies to sardines and back: Multidecadal change in the Pacific Ocean, *Science*, *299*, 217–221.

Colwell, R. R. (1996), Global climate and infectious disease: The cholera paradigm, *Science*, *274*, 2025–2031.

Fu, X., B. Wang, T. Li, and J. McCreary (2003), Coupling between northward-propagating boreal summer ISO and Indian Ocean SST: Revealed in an atmosphere-ocean coupled model, *J. Atmos. Sci.*, *60*, 1733–1753.

Gildor, H., A. H. Sobel, M. A. Cane, and R. N. Sambrotto (2003), A role for ocean biota in tropical intraseasonal atmospheric variability, *Geophys. Res. Lett.*, *30*(9), 1460, doi:10.1029/2002GL016759.

Hendon, H. H., and J. Glick (1997), Intraseasonal air-sea interaction in the tropical Indian and Pacific Oceans, *J. Clim.*, *10*, 647–661.

Hendon, H. H., and M. L. Salby (1994), The life-cycle of the Madden-Julian Oscillation, *J. Atmos. Sci.*, *51*, 2225–2237.

Hendon, H. H., B. Liebmann, and J. D. Glick (1998), Oceanic Kelvin waves and the Madden-Julian oscillation, *J. Atmos. Sci.*, *55*, 88–101.

Kemball-Cook, S., and B. Wang (2001), Equatorial waves and air-sea interaction in the Boreal summer intraseasonal oscillation, *J. Clim.*, *14*, 2923–2942.

Lau, W. K. M., and D. E. Waliser (Eds.) (2005), *Intraseasonal Variability of the Atmosphere-Ocean Climate System*, 474 pp., Springer, New York.

Lehodey, P., M. Bertignac, J. Hampton, A. Lewis, and J. Picaut (1997), El Nino–Southern Oscillation and tuna in the western Pacific, *Nature*, *389*, 715–718.

Lehodey, P., F. Chai, and J. Hampton (2003), Modelling climate-related variability of tuna populations from a coupled ocean-biogeochemical-populations dynamics model, *Fish Oceanogr.*, *12*, 483–494.

Lobitz, B., L. Beck, A. Huq, B. Wood, G. Fuchs, A. S. G. Faruque, and R. Colwell (2000), Climate and infectious disease: Use of remote sensing for detection of *Vibrio cholerae* by indirect measurement, *Proc. Natl. Acad. Sci. U. S. A.*, *97*, 1438–1443.

Madden, R. A., and P. R. Julian (1994), Observations of the 40–50-day tropical oscillation: A review, *Mon. Weather Rev.*, *122*, 814–837.

McClain, C. R., G. C. Feldman, and S. B. Hooker (2004), An overview of the SeaWiFS project and strategies for producing a climate research quality global ocean bio-optical time series, *Deep Sea Res., Part II*, *51*, 5–42.

McCreary, J. P., K. E. Kohler, R. R. Hood, S. Smith, J. Kindle, A. S. Fischer, and R. A. Weller (2001), Influences of diurnal and intraseasonal forcing on mixed-layer and biological variability in the central Arabian Sea, *J. Geophys. Res.*, *106*, 7139–7155.

Murtugudde, R. G., S. R. Signorini, J. R. Christian, A. J. Busalacchi, C. R. McClain, and J. Picaut (1999), Ocean color variability of the tropical Indo-Pacific basin observed by SeaWiFS during 1997–1998, *J. Geophys. Res.*, *104*, 18,351–18,366.

Murtugudde, R., J. Beauchamp, C. R. McClain, M. Lewis, and A. J. Busalacchi (2002), Effects of penetrative radiation on the upper tropical ocean circulation, *J. Clim.*, *15*, 470–486.

Nakamoto, S., S. P. Kumar, J. M. Oberhuber, J. Ishizaka, K. Muneyama, and R. Frouin (2001), Response of the equatorial Pacific to chlorophyll pigment in a mixed layer isopycnal ocean general circulation model, *Geophys. Res. Lett.*, *28*, 2021–2024.

Pascual, M., X. Rodo, S. P. Ellner, R. Colwell, and M. J. Bouma (2000), Cholera dynamics and El Nino-Southern Oscillation, *Science*, *289*, 1766–1769.

Siegel, D. A., J. C. Ohlmann, L. Washburn, R. R. Bidigare, C. T. Nosse, E. Fields, and Y. M. Zhou (1995), Solar-radiation, phytoplankton pigments and the radiant heating of the equatorial Pacific warm pool, *J. Geophys. Res.*, *100*, 4885–4891.

Strutton, P. G., and F. P. Chavez (2000), Primary productivity in the equatorial Pacific during the 1997–1998 El Niño, *J. Geophys. Res.*, *105*, 26,089–26,101.

Waliser, D. E. (2005), Intraseasonal variability, in *The Asian Monsoon*, edited by B. Wang, Springer, New York, in press.

Waliser, D. E., K. M. Lau, and J. H. Kim (1999), The influence of coupled sea surface temperatures on the Madden-Julian oscillation: A model perturbation experiment, *J. Atmos. Sci.*, *56*, 333–358.

Waliser, D. E., R. Murtugudde, and L. E. Lucas (2003a), Indo-Pacific Ocean response to atmospheric intraseasonal variability: 1. Austral summer and the Madden-Julian Oscillation, *J. Geophys. Res.*, *108*(C5), 3160, doi:10.1029/2002JC001620.

Waliser, D. E., K. M. Lau, W. Stern, and C. Jones (2003b), Potential predictability of the Madden-Julian Oscillation, *Bull. Am. Meteorol. Soc.*, *84*, 33–50.

Wiggert, J. D., R. G. Murtugudde, and C. R. McClain (2002), Processes controlling interannual variations in wintertime (northeast Monsoon) primary productivity in the central Arabian Sea, *Deep Sea Res., Part II*, *49*, 2319–2343.

Xie, P. P., and P. A. Arkin (1997), Global precipitation: A 17-year monthly analysis based on gauge observations, satellite estimates, and numerical model outputs, *Bull. Am. Meteorol. Soc.*, *78*, 2539–2558.

Zheng, Y., D. E. Waliser, W. F. Stern, and C. Jones (2004), The role of coupled sea surface temperatures in the simulation of the Tropical Intraseasonal Oscillation, *J. Clim.*, *17*, 4109–4134.

J.-L. Li and D. E. Waliser, Jet Propulsion Laboratory, California Institute of Technology, 4800 Oak Grove Drive, MS 183-501, Pasadena, CA 91109, USA. (duane.waliser@jpl.nasa.gov)

R. Murtugudde, Earth System Science Interdisciplinary Center, University of Maryland, Room 2201, College Park, MD 20742, USA.

P. Strutton, College of Oceanic and Atmospheric Sciences, Oregon State University, 104 Ocean Admin Bldg., Corvallis, OR 97331-5503, USA.